17th World Conference on Earthquake Engineering, 17WCEE
Sendai, Japan - September 13th to 18th 2020

RELATIONS BETWEEN THE CRUSTAL STRAINS AND DAMAGE TO GROUND CAUSED BY THE 2016 KUMAMOTO EARTHQUAKE, JAPAN

M. Kamiyama[(1)], A. Mikami[(2)], H. Koide[(3)], Y. Sawada[(4)], H. Akita[(5)] , N. Chiba[(6)]

[(1)] *Prof. Emeritus, Department of Civil Engineering, Tohoku Institute of Technology, mkamiyam@tohtech.ac.jp*
[(2)] *Prof., Department of Civil Engineering, Tokai University, atsushi.mikami@tokai.ac.jp*
[(3)] *Prof., Department of Civil Engineering, Tohoku Institute of Technology, koide@tohtech.ac.jp*
[(4)] *Prof. Emeritus, Tohoku University, yasuji.sawada.a4@tohoku.ac.jp*
[(5)] *Prof. Emeritus, Department of Civil Engineering, Tohoku Institute of Technology, hakita@tohtech.ac.jp*
[(6)] *Prof., Department of Civil Engineering, Tohoku Institute of Technology, nchiba@tohtech.ac.jp*

Abstract

Most of current analyses for earthquake damage focus on acceleration motions subjected to structures. The reason is that earthquake damage has been considered to attribute to inertia force subjected to structures. However, earthquake damage depends on types of structures and acceleration motions are not necessarily unique seismic force controlling damage. The 2016 M_w7.1 Kumamoto Earthquake, Japan provided a useful opportunity to investigate the relations between earthquake damage to various kinds of structures and different types of seismic forces. This paper presents the crustal deformations due to the earthquake based on the data observed by GEONET, GNSS Earth Observation Network as well as the seismic intensity using strong acceleration-motion records by K-NET and KiK-net. Both parameters of the co-seismic strains of ground and seismic intensity are compared with damage data of civil engineering structures. Emphasis is placed here on comparisons between the co-seismic strains and damage to soil structures such as ground slope. The concluding remarks of this paper are summarized as follows: (1) The 2016 Kumamoto Earthquake caused great crustal deformations near its epicenter, recording about1000mm in the horizontal component and about 270 mm in the vertical. (2) The co-seismic strains of ground were estimated by the spatial differentiation for the crustal displacements observed by the GEONET system using a FEM technique. They were finally summarized to the two strain invariants of engineering maximum shear strain and dilatation strain and mapped in the Kumamoto Prefecture area. Both parameters of strains showed a quite peculiar pattern of distribution reflecting the seismic source mechanism. (3) The seismic intensity according to the JMA definition was also estimated using the strong acceleration motions observed by the K-NET and KiK-net systems and mapped in the Kumamoto Prefecture area being compared with the distributions of the co-seismic strains of ground. The seismic intensity distribution has a quite different feature from the ones of co-seismic strains of ground. (4) In order to clarify the effects of both parameters of co-seismic strains of ground and seismic intensity on structural damage caused by the earthquake, a comprehensive and integrated investigation result over damage to soil structures conducted by the Geospatial Information Authority of Japan, GSI was cited here with the positional data for the 1044 damage sites in total. Comparisons of the GSI's result with the distributions of co-seismic strains of ground and seismic intensity revealed that there is a remarkable difference between the distributions of seismic intensity and of the damage sites while the majority of the damage sites overlaps with the peak value areas of co-seismic strains of ground. (5) This paper finally concludes that we should pay attention not only to acceleration motions but also to geodetic effects to more comprehensively deal with seismic forces responsible for earthquake damage.

Keywords: The 2016 Kumamoto Earthquake, GNSS, crustal deformations, crustal strains, damage to ground

1. Introduction

On April 14, 2016 at 21:26 JST and on April 16, 2016 at 01:25 JST, two large earthquakes consecutively struck the Kumamoto area of Kyushu Island in Japan, respectively, with a magnitude of M_w 6.2 (M_J 6.5) and a magnitude of M_w7.1 (M_J 7.3), causing fatal victims of death and missing people reaching more than 250 and badly damaging various kinds of structures [1]. The earthquakes are all together named the 2016 Kumamoto Earthquake by the Japan Meteorological Agency (JMA); the former is called the largest foreshock and the latter the mainshock of the earthquake [1].

The disastrous earthquake, which is classified as an inland crustal earthquake according to the seismological terms in Japan [1] , has a character to be elaborately monitored by various kinds of observation systems deployed around the epicenter. Fig.1(a) shows a map of sites, where strong ground motions and crustal movements were observed during the earthquake, together with the epicenters of the largest foreshock and mainshock. The observation systems of strong ground motions here consist of K-NET and KiK-net that are both installed and administered by the National Research Institute for Earth Science and Disaster Resilience (NIED) [2]. Another observation system shown in Fig.1(a) is GEONET(GNSS Earth Observation Network) that is a comprehensive system for positioning and monitoring crustal deformations of the Japanese Islands using the GNSS technology (continuous GNSS) [3]. The observation system was installed by the Geospatial Information Authority of Japan, GSI almost at the same time of the installations of K-NET and KiK-net. Nowadays GEONET observation stations have been deployed at over 1,300 sites throughout Japan and their various kinds of observed and produced data are widely available to the public through GSI [3].

The 2016 Kumamoto Earthquake provides a valuable opportunity to investigate the relations between damage to various kinds of structures and different types of seismic forces because of the data availability. In particular, this earthquake produced rich data of ground offset (ground permanent displacements) by GEONET that have not been fully obtained during earthquakes in the past. The data by K-NET and KiK-net present information of acceleration while GEONET can give information of geodetic deformation such as ground permanent displacement, so the 2016 Kumamoto Earthquake might be best to identify their respective roles for earthquake damage. Until nowadays, earthquake damage has been considered to be mainly attributable to inertia force due to acceleration. Although inertia force exerts some significant effects on earthquake damage, it is still a scientific concern to find what kind of physical force is essential to earthquake damage to structures [4].

The purpose of this paper is to investigate the geodetic effects on earthquake damage to soil structures based on various kinds of data obtained during the 2016 Kumamoto Earthquake. We especially place emphasis on the effects of crustal strains, which are numerically derived from the observed displacement offsets through GEONET, to relate with earthquake damage to soil structures. Such relations were similarly investigated by the authors for other damaging earthquakes [5]. In this paper, we intend to compare them with the results from the 2016 Kumamoto Earthquake and discuss comprehensively the geodetic effects on earthquake damage.

2. Strong ground motions and crustal deformations due to the earthquake

Fig.1(b) shows a distribution map of earthquakes that occurred for a period from the time of the largest foreshock to April 17 at 24:00 JST: about one day after the mainshock, citing seismic source data from JMA [1] . The epicenters of earthquakes including the largest foreshock, mainshock and one-day aftershocks extend almost linearly in the southwest-northeast direction. This distribution of earthquakes might provide a projection on the ground surface for the seismic source faults associated with the 2016 Kumamoto Earthquake. Fig.2, on the other hand, shows a distribution map of the JMA seismic intensity numerically derived using the acceleration records observed at the ground surface during the mainshock by the K-NET and KiK-net systems shown in Fig.1(a). In Fig.2, the seismic intensity scales are expressed as a color image with contour lines together with the epicenter of the mainshock and the demarcation lines of towns, cities and prefectures. The distribution of seismic intensity in Fig.2 indicates an extensive tendency of distribution in the southwest-

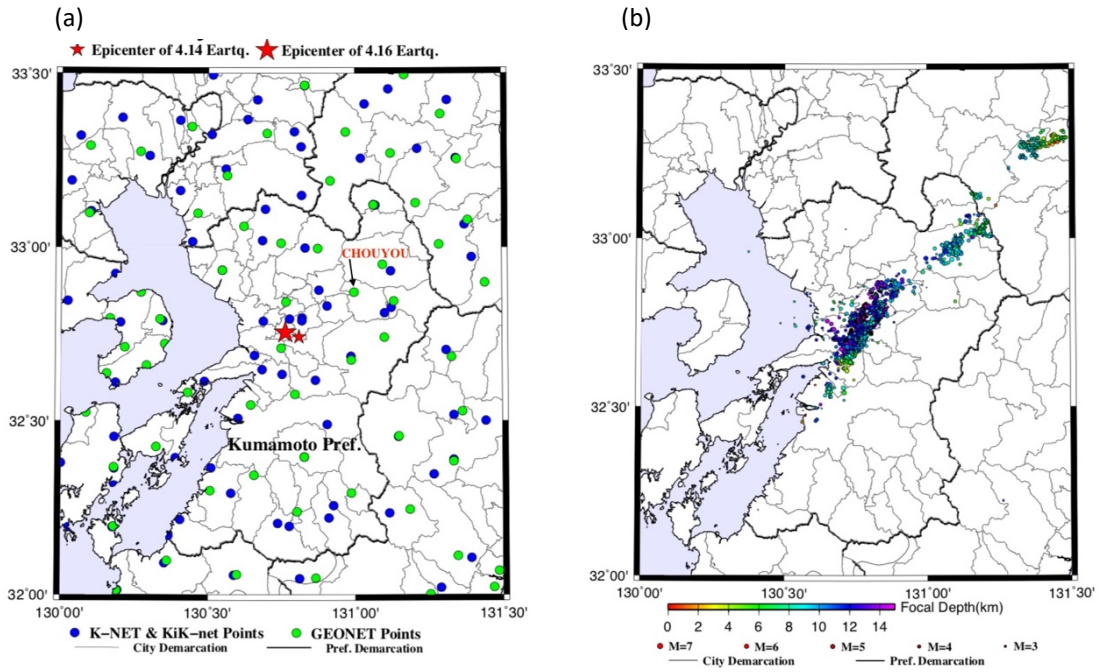

Fig. 1 Maps of observation stations and distribution of earthquakes
(a) Map of observation stations
(b) Map of distribution of earthquakes

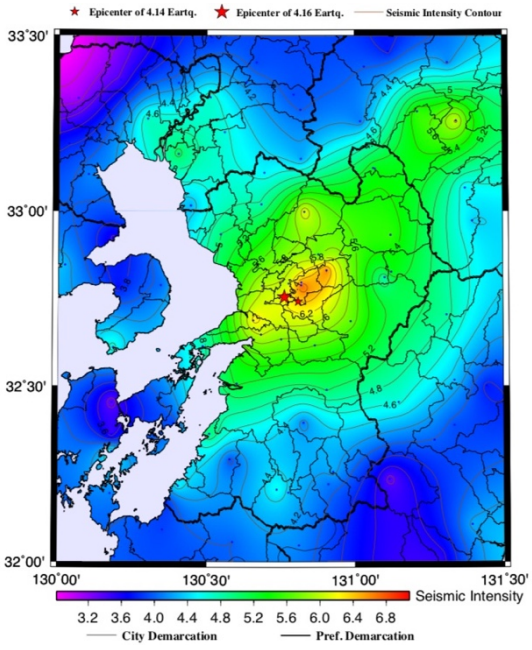

Fig. 2 Distribution of seismic intensity due to the mainshock

northeast direction almost consistently with the earthquake distribution in Fig.1(b). In addition, Fig.2 shows that the largest intensity distributes in an area slightly far from the epicenter of the mainshock to the northeast direction.

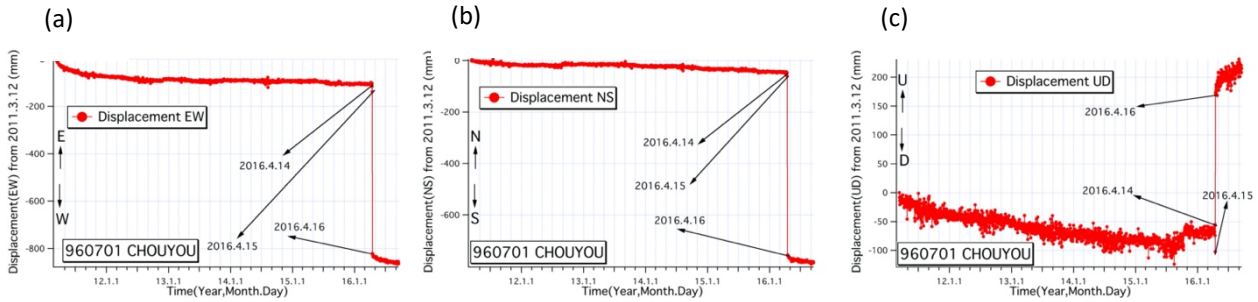

Fig. 3 Daily variations of crustal displacements at the CHOUYOU station of GEONET where the co-seismic maximum displacement was recorded during the mainshock. (a) EW component (b) NS component (c) UD component

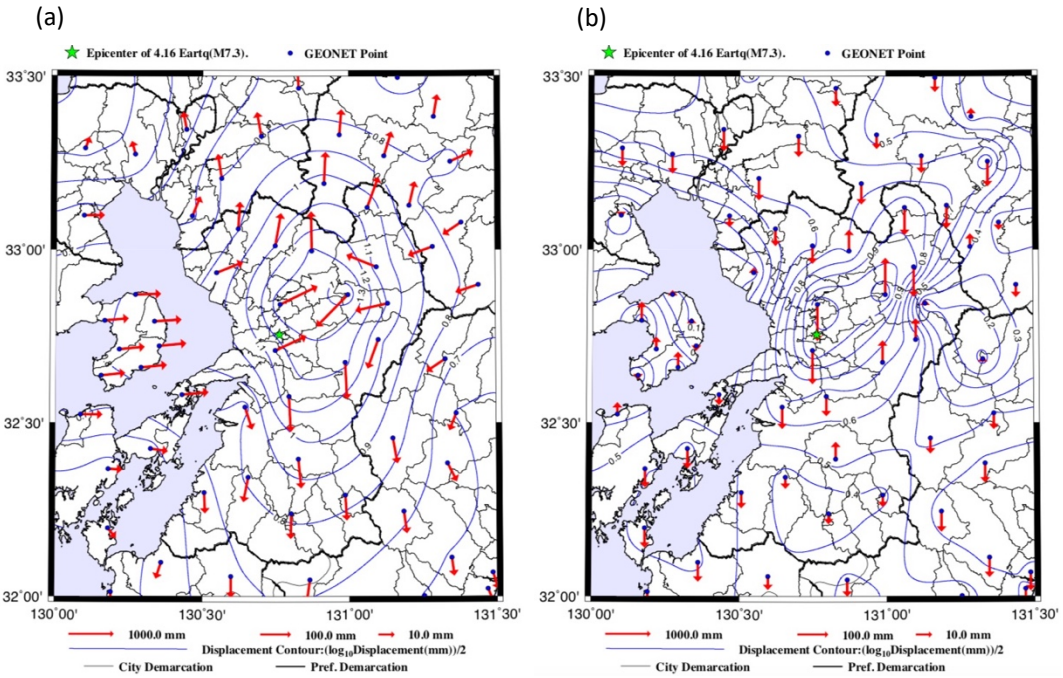

Fig. 4 Distributions of co-seismic crustal movements (a) Horizontal component (b) Vertical component

GEONET also observed crustal deformations, which are significant seismic force parameter different from strong ground acceleration motions, during the pre-, co- and post-seismic periods of the 2016 Kumamoto Earthquake. Fig.3 shows, as an example, daily variations of displacements in the east-west, north-south and up-down directions recorded from March 12, 2011 to September 17, 2016 at the CHOUYOU observation station of GEONET shown in Fig.1(a) where the maximum value of the co-seismic movements was observed during the mainshock. We obtained co-seismic crustal movements due to the mainshock at each observation station of GEONET by calculating the differences of displacements between on April 15 and on April 16 in the temporal records as shown in Fig.3. Fig.4 shows the distributions of horizontal and vertical vectors for the obtained co-seismic crustal movements. Both vectors of crustal movements are plotted in terms of logarithmic scale divided by a constant value to avoid overlapping of vector traces and to clearly express their directions and absolute values that range broadly from a large level of meter to a small one of millimeter. The standard scale of logarithmic values is shown in Fig.4. At the same time, contour lines of absolute values are plotted in

Fig.4 to clearly show the distribution trend. Note here that the contour lines are scaled by taking the logarithm of displacement (mm) and dividing the logarithmic value by a constant of 2. The epicenter of the mainshock is also plotted in Fig.4. The maximum values of co-seismic crustal movements near the epicenter are found to be about 1000 mm and 270 mm, respectively, in the horizontal and vertical components. In addition, the co-seismic crustal movements near the epicenter show a characteristic distribution probably reflecting the seismic faulting mechanism of the mainshock. The crustal movements in the horizontal component near the epicenter indicate directional traces of a right-lateral strike-slip mechanism compatible with the information by JMA [1] and their contour lines tend to expand in the north-south direction with an elliptic form. For the vertical component, on the other hand, its contour lines have a tendency to extend from the southwest to the northeast directions consistently with the distribution of earthquakes shown in Fig.1(b). Thus, the distribution patterns of both components are different from each other; the horizontal tends to reflect the mechanical factors of seismic source faulting while the vertical has a comparatively high relation with the spatial configuration of seismic source faulting.

3. Estimate of co-seismic crustal strains due to the earthquake

The above-described seismic intensity and co-seismic crustal movement might exert different effects on structures depending on their respective characters; the former mainly results from acceleration while the latter is related with displacement. Especially the latter culminates in strains or stresses that finally induce some mechanical effects on structures differently from acceleration. In this section, we focus on the estimates of ground strains that are numerically obtained by the spatial differential calculus from co-seismic crustal movements. Such ground strains are called here "the co-seismic strains of ground."

The co-seismic strains of ground have been long recognized to be significant for seismic behaviors of underground structures such as buried pipelines while they have been less associated with conventional aboveground structures where the inertial effects are of primary interest [4]. The 1995 Kobe Earthquake, however, provided an opportunity to reconsider such a situation. The earthquake caused disastrous damage to various kinds of civil engineering structures and highlighted the effects of co-seismic strains of ground as another key factor controlling damage. The Japan Society of Civil Engineers thus issued a proposal placing emphasis on the effects of co-seismic strains of ground on civil engineering structures including aboveground ones [4]. The co-seismic strains of ground, however, are rather difficult to observe compared with other seismic parameters such as acceleration. Especially they have not been directly obtained during damage-causing earthquakes in Japan. This situation makes it difficult to discuss their effects on earthquake damage to civil engineering structures. Relating with this problem, the GEONET system is extremely useful to break through such dilemma. As stated above, GEONET has provided displacement data possible to numerically obtain co-seismic strains of ground due to damage-causing earthquakes that occurred in Japan since its installation.

The GEONET system provides three-dimensional displacements on the ground surface at its each observation station as shown in Fig.4. In this paper, we only focus on the two-dimensional(2-D) strains obtained on the ground surface plane from the horizontal components of displacements omitting the vertical component of displacement because the observation of displacements here is limited on the ground surface without the vertical-direction deployment of observation. When two-directional displacements in the east-west(EW) and north-south(NS) directions are available at discrete points on the ground surface, 2-D strains within the body surrounded by the points can be obtained using the spatial differential calculus for the displacements based on a theory of the plane strain condition [6]. We used here a Finite Element Method (FEM) composed of triangular elements[6]. The FEM technique gives the normal strains ε_{EW} and ε_{NS} in respective directions of EW and NS and shear strain γ_{NE} on the EW-NS plane using the two-directional displacements u and v in the NS and EW axes. From these strain components, we estimated the maximum principal strain ε_{max} and minimum principal strain ε_{min} by the tensor transform. Finally, we estimated the engineering maximum shear strain γ_{max} and dilatation strain $\varepsilon_{dilatation}$, which both correspond to the two invariants for the mathematical transform of 2-D strain tensor, and the principal direction of strains on the EW-NS plane to represent the strain characteristics in each triangle element as follows:

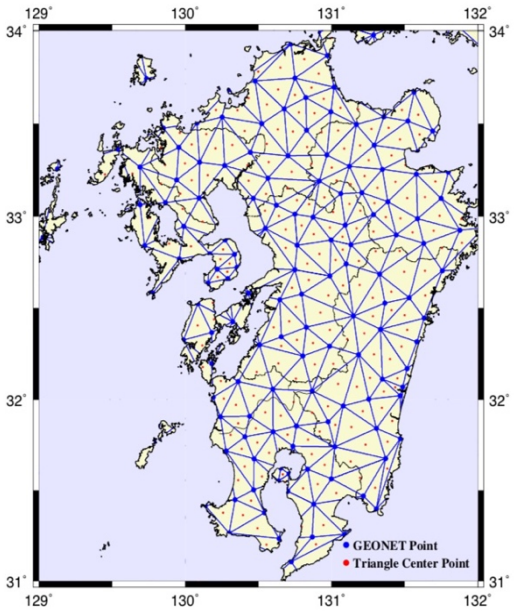

Fig. 5 Triangle net produced by the Delaunay method for the GEONET stations

$$\gamma_{max} = \varepsilon_{max} - \varepsilon_{min} \quad (1)$$

$$\varepsilon_{dilatation} = \varepsilon_{max} + \varepsilon_{min} \quad (2)$$

Note here that the present FEM method provides strains smoothed over the GEONET's station-to-station distance of some 20 km and gives less information on strains within more local areas over some 10 meters' level. Even such strains by the present method, however, are meaningful in the analyses of relative vulnerability of structures because their absolute maximum values generally tend to be proportional to the maximum of the local strains in the same ground area [7]. At the same time, strains here are not dynamic but static because they are derived from permanent (static) displacements. It is needless to say that earthquake damage actually results from the dynamic effects of oscillating strains during earthquakes. Even so, the strains obtained by the present method might be useful to detect a barometer for the damage potential to structures, because they have a proportional relation with the absolute peaks of oscillating strains [7]. The present method thus might provide an index reliable enough to indirectly represent the vulnerability of structures during earthquakes.

In order to perform FEM of triangular elements, it is first necessary to constitute a triangle net for the randomly scattered observation stations of GEONET. We used the Delaunay triangulation method for the purpose [8]. Fig.5 shows a triangle-net system obtained by the method for the GEONET observation stations. The centers of the triangles were used to represent the strains estimated in each triangular element. Fig.6 shows distributions of the co-seismic engineering maximum shear strains and co-seismic dilatation strains estimated in each triangular element during the mainshock. We used a technique of the GMT software [9] to smoothly plot the distributions of strains in Fig6. Both figures in Fig6 present the distributions as a color image with contour lines of strains. Note here that the engineering maximum shear strains in Fig.6 are transformed into the logarithmic scale to reasonably express the broad-ranged absolute values while the dilatation strains in Fig.6 are normal to express the values changeable from minus to plus. The estimated orientations of the principal strain axes are also plotted in both figures. In addition, the epicenters of the mainshock and the largest foreshock are shown in the figures to identify the positional relation between the distribution of strains and earthquake source. Fig.6 clearly demonstrates that the maximum shear strains and dilatations have both an extremely characteristic distribution probably in response to the seismic faulting mechanism of source. The engineering maximum shear strains, for example, concentrate their greater values in an area far from the epicenters in the north-east direction whereas the dilatation strains scatter distinctively and regularly with the

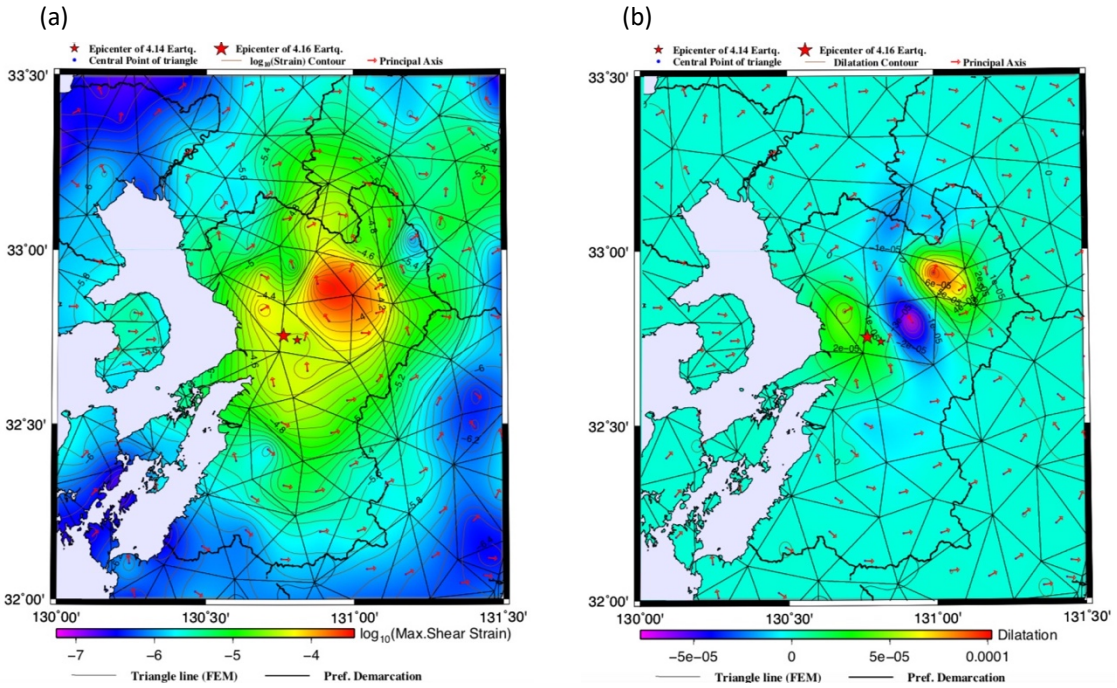

Fig. 6 Distribution of the co-seismic strains of ground
(a) Distribution of engineering maximum shear strains
(b) Distribution of dilatation strains

domains of minus value(compression) and plus value (dilatation) around the mainshock's epicenter. A comparison of Fig.6 with Fig.2 indicates that the distributions of co-seismic strains of ground differ remarkably from the one of seismic intensity. Especially, there is a marked difference in their distributions between the seismic intensity in Fig.2 and engineering maximum shear strain in Fig.6 from a viewpoint of the concentration degree of the maximum values.

4. Damage caused by the earthquake and their relations with seismic forces

The 2016 Kumamoto Earthquake caused tremendous damage extended mainly in the Kumamoto Prefecture area. Many various institutes and researchers investigated damage to different kinds of structures ranging from private residential houses to public infrastructures from their respective standpoints of interest. Among these investigations, which were compiled into a great number of reconnaissance reports, the investigation over the damage to soil structures including natural slopes of ground conducted by GSI is interesting and valuable because it was carried out systematically according to an integrated manner [10]. Immediately after the earthquake, GSI made an attempt to comprehensively identify damage sites to soil structures including slope failure, landslide and debris-avalanche using the aerial photograph technology for the sake of providing information about the restoration and revival for seismic damage due to the earthquake. GSI finally compiled a reconnaissance report composed of numerical positions of latitude and longitude for the damage sites [10]. The GSI investigation covered evenly a wide-ranged area mainly including the Kumamoto Prefecture district and the number of the damage sites amounts to 1,044 in total. All of these damages are reliable enough to cite because they were confirmed through field works by the prefectural office of Kumamoto. Fig.7 shows a map of damage sites resulting from the GIS investigation plotted together with the altitude of ground. Fig.7 illustrates that most of the damage sites scatter around areas far from the epicenter showing a tendency to concentrate on the northeastern area rather than on the epicentral area. At the same time, the damage sites are seen to have a relation with the topography of ground; they tend to scatter around Mount Aso which is one of

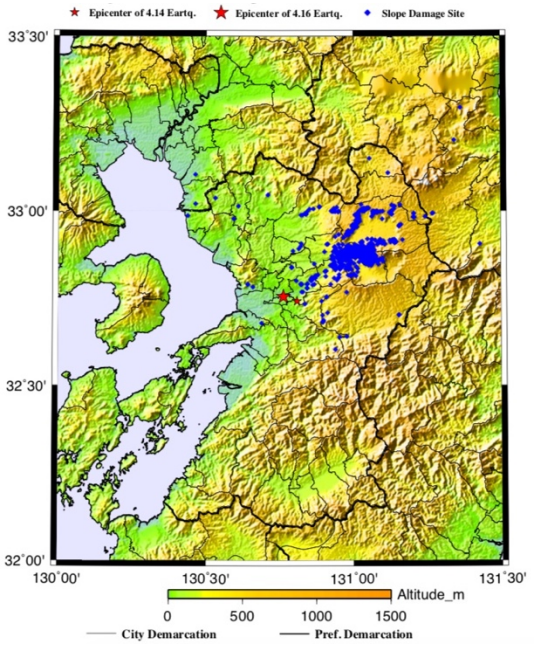

Fig. 7 Map of damage sites to soil structures cited from the GSI investigation. The blue diamonds are the damage sites to soil structures. Altitudes are given as a color image in terms of meter to express topography.

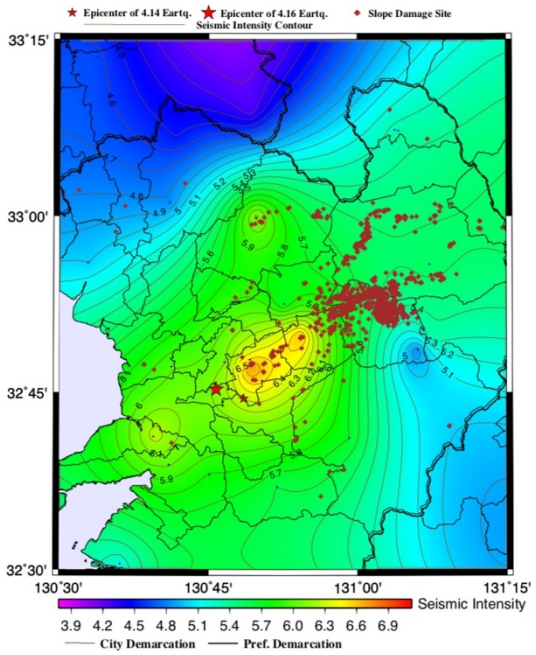

Fig.8 Map of comparative distributions between seismic intensity and damage sites to soil structures

the largest active volcanoes in the world with a large caldera. The local site conditions including the topography of ground might thus affect the damage compiled by GSI together with various seismic forces triggered during the earthquake. We here focus only on the effects of seismic forces on the damage phenomena, as a case study on the interdependence between seismic forces and earthquake damage.

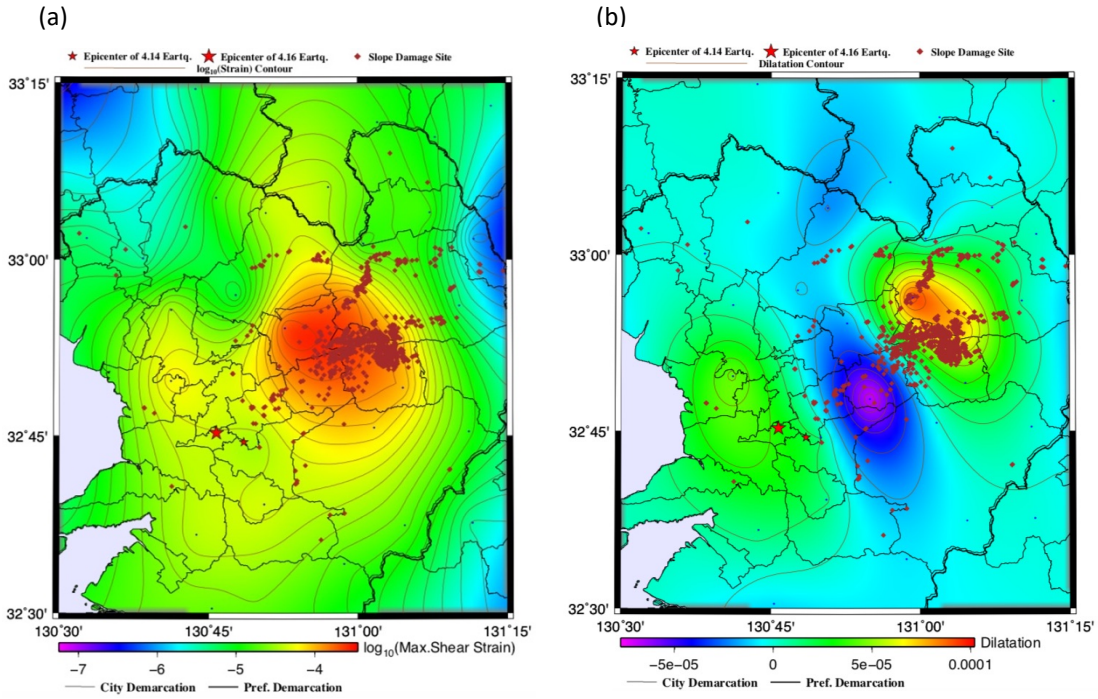

Fig.9 Maps of comparative distributions between co-seismic strains of ground and damage sites to soil structures

(a) Map of comparative distributions between engineering maximum shear strains and damage sites to soil structures

(b) Map of comparative distributions between dilatation strains and damage sites to soil structures

In order to compare the damage compiled by GSI with two types of seismic forces of seismic intensity scale and co-seismic strains of ground, we overlapped the damage sites on the distribution maps of seismic intensity, engineering maximum shear strain and dilatation strain, as shown in Figs.8 and 9. Fig.8 indicates a remarkable difference between the distribution of seismic intensity and the one of damage sites; most of the damage sites are separated from the peak area of seismic intensity and distributed mainly in a comparatively low area of seismic intensity. Contrary to such a difference, the damage sites almost concentrate on the peak areas of engineering maximum shear strains and dilatation strains in Fig.9, showing a good correlation between damage to soil structures and co-seismic strains of ground. Fig.9 also clarifies that the damage sites are located almost within an area having engineering maximum shear strains of over $10^{-4.5}$ (some 0.00003). The engineering maximum shear strain, as is well known, is a mechanical parameter to effectively decide the failure of structures and the value of $10^{-4.5}$ (some 0.00003) thus presents an example of vulnerability limit of soil structures in terms of engineering maximum shear strain.

To obtain a statistical relation between damage to soil structures and engineering maximum shear strains, a histogram analysis was made for the distribution in Fig.9. We here estimated the value of engineering maximum shear strain at the latitude and longitude relevant to the damage site using an interpolation method provided in the GMT software [9] from the original distribution of engineering maximum shear strains. Figure 10 shows the analyzed histogram illustrating a correlation between the number of damage sites and the value of engineering maximum shear strains. It is seen in Fig.10 that there is a generally proportional trend between the number of damage and the value of engineering maximum shear strain. We can also find a threshold value of engineering maximum shear strain in Fig.10 to determine where soil structures are vulnerable; most of soil structures are possibly vulnerable at places where the engineering maximum shear strain exceeds

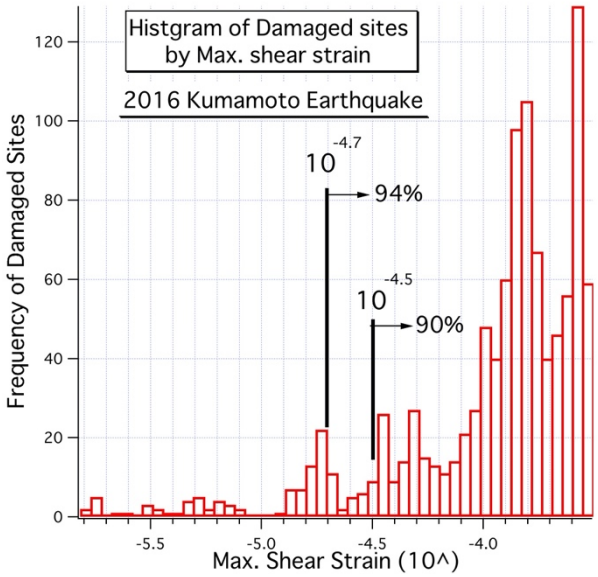

Fig.10 Histogram analyzed from the engineering maximum shear strains and damage sites to soil structures due to the 2016 Kumamoto Earthquake

approximately $10^{-4.7}(0.00002) \sim 10^{-4.5}(0.00003)$. This value of vulnerability limit agrees well with the results similarly analyzed for civil engineering structures including soil structures for other large earthquakes. See Kamiyama et al. for more detailed results [5].

5. Concluding remarks

The 2016 Kumamoto Earthquake presented a useful opportunity to investigate the correlation between structural damage and seismic forces to be differently effective to structures. As representative seismic forces, we here focused on two parameters; the first is the seismic intensity scale numerically derived from acceleration data observed by both systems of K-NET and KiK-net and the second the co-seismic strains of ground obtained by the spatial differential calculus for the observed crustal displacements from GEONET. The results of this research are summarized as follows:

The co-seismic strains of ground estimated by the spatial differentiation for the crustal displacements observed by the GEONET system using a FEM technique showed a quite peculiar pattern of distribution reflecting the seismic source mechanism that elementary sources on the fault plane propagated from its hypocenter toward the north-east direction. As a result of such mechanism, the peak values of the co-seismic strains of ground concentrated on the northeastward area, where large-scale infrastructures including landslides suffered severe damage, being far from the epicenter

The seismic intensity estimated using the strong acceleration motions by the K-NET and KiK-net systems was compared with the distributions of the co-seismic strains of ground. The distribution of seismic intensity showed a characteristic feature related similarly with seismic source mechanism, having its peak value in an area in the northeast direction slightly far from the epicenter. However, the seismic intensity distribution has a quite different feature from the ones of co-seismic strains of ground, being more consistent with the distribution trend of damage to residential houses rather than with damage to large-scale infrastructures.

In order to clarify the effects of both parameters of co-seismic strains of ground and seismic intensity on structural damage by the earthquake, a comprehensive and integrated investigation result over damage to soil structures conducted by GSI was cited here. Comparisons of the GSI's result with the distributions of co-

seismic strains of ground and seismic intensity revealed that there is a remarkable difference between the distributions of seismic intensity and of the damage sites while the majority of the damage sites overlaps with the peak value areas of co-seismic strains of ground. This comparison result is compatible with the investigations made by the authors for the past damage-causing earthquakes: civil engineering structures including soil structures are more vulnerable to co-seismic strains of ground rather than to seismic intensity that has a strong relation with acceleration.

The histogram analysis for the relation between the number of damage sites and the values of engineering maximum shear strain based on the GSI investigation made it clear that civil engineering structures including soil structures are prone to suffer damage at places where the engineering maximum shear strain exceeds a threshold value of some $10^{-4.7}(0.00002) \sim 10^{-4.5}(0.00003)$. This value of vulnerability limit agrees well with the results similarly analyzed for the 2011 Great East Japan Earthquake and the 2008 Iwate-Miyagi Inland Earthquake [5].

The damage experiences and observed data through the 2016 Kumamoto Earthquake concludes that the geodetic effect on earthquake damage to civil engineering structures is by no means negligible; on the contrary, emphasis should be placed on the effect, especially on the co-seismic strains of ground. It is expected that geodetic data resulting from the GNSS technique like GEONET are more used in the earthquake engineering field, where less attention has been paid to geodesy, to comprehensively deal with seismic forces responsible for earthquake damage.

6. References

[1] Japan Meteorological Agency, JMA (2018): Report on the 2016 Kumamoto Earthquake, Technical Report of the Japan Meteorological Agency No.135, ISSN 0447-3868, 1-305 (in Japanese).

[2] NIED, National Research Institute for Earth Science and Disaster Prevention, Home Page (2020), http://www.k-net.bosai.go.jp/.

[3] GSI. Geospatial Information Authority of Japan. Home Page (2020), http://www.gsi.go.jp.

[4] Japan Society of Civil Engineers (1995): Proposal on earthquake resistance for civil engineering structures. JSCE Magazine Civil Engineering, 80, 1-7 (in Japanese).

[5] Kamiyama, M, Koide, H, Sawada, Y, Akita, H, Chiba, N. (2017): Monitoring of crustal deformations and its application to mitigation of earthquake disasters. Journal of JSCE (Japan Society of Civil Engineers) Division A, Structural Engineering/Earthquake Engineering & Applied Mechanics;5:1206-225.

[6] Zienkiewicz, OC, Cheung, Y.K. (1967): The finite element in structural and continual mechanics. McGraw-Hill House.

[7] Trifunac, MD, Todorovska, MI. (1997): Northridge, California, earthquake of 1994: density of pipe breaks and surface strains. Soil Dynamics and Earthquake Engineering. 16:193-207.

[8] Lee, DT, Schachter, BJ. (1980): Two algorithms for con-structing a Delaunay triangulation. International Journal of Computer and Information Sciences. 91: 219-242.

[9] Wessel, P, Smith, WHF. (1999): The generic mapping tools. Technical Reference and Cookbook. Version 3.3: 1-132.

[10] GSI, Geospatial Information Authority of Japan (2016): Information on the 2016 Kumamoto Earthquake. http://www.gsi.go.jp/BOUSAI/H27-kumamoto-earthquake-index.html.

